Ray tracing for anisotropic media in singular directions of S waves

Václav Vavryčuk

Institute of Physics, Federal University of Bahia, 40210-340 Salvador, Bahia, Brazil. E-mail: vaclav@ufba.br
On leave from: Geophysical Institute, Academy of Sciences of the Czech Republic, Boční II/1401, 141 31 Praha 4, Czech Republic. E-mail: vv@ig.cas.cz

SUMMARY

S-wave singularities often cause troubles to tracing of rays in inhomogeneous anisotropic media. The ray tracing algorithms can breakdown in the vicinity of the singularities, because the medium becomes nearly degenerate and the right-hand sides of the ray tracing equations yield indefinite expressions. We propose a modified ray-tracing approach, which is numerically stable and yields correct results in all kinds of singularities and their vicinities. We show applicability and efficiency of this approach on various numerical examples. We discuss a possibility of splitting of a ray when crossing a singularity.

1 INTRODUCTION

S-wave singularities are very common in all kinds of anisotropy and often cause troubles in tracing of rays in inhomogeneous anisotropic media. They also cause anomalies in the polarization of a wavefield and in the geometry of wave surfaces (Alshits & Lothe 1979; Alshits, Sarychev & Shuvalov 1985; Crampin & Yedlin 1981; Grechka & Obolentseva 1993; Helbig 1994; Vavryčuk 1999). They are defined as the directions where two S waves have coincident phase velocities, hence the medium is degenerate in this direction. We distinguish between kiss, intersection and point singularities. The point singularity is also called the conical point and is probably the most complicated singularity affecting geometry of rays and the wavefield in the most striking way (Miller & Musgrave 1956; Burridge 1967; Musgrave

1985; Grechka & Obolentseva 1993; Rümpker & Thomson 1994). All these singularities can appear in weakly as well as in strongly anisotropic media. In strong anisotropy they usually appear together with the so-called triplications, which also complicate geometry of the wavefront. However, the triplications do not pose complications to the ray-tracing equations, while the singularities can cause breakdowns of the ray-tracing algorithms (Shearer & Chapman 1989; Červený 2000; Pšenčík & Dellinger 2000). These breakdowns are connected to numerical instabilities that arise whenever the phase velocity sheets of two waves are close to each other. The medium becomes nearly degenerate and the right-hand sides of the ray-tracing equations yield indefinite expressions (Gajewski & Pšenčík 1990). It results in an inaccurate or even erroneous ray tracing or in a collapse of the algorithm.

In this paper we shall show that these difficulties are not essential and can be overcome by formulating a proper ray tracing strategy. This strategy is based on the inspection of behaviour of polarization vector of the traced wave whenever the ray approaches the singularity. This strategy can be easily coded and needs only a slight modification of existing ray tracers. On numerical examples we show applicability and efficiency of our approach. We discuss a possibility of splitting of the ray, which crosses the singularity.

2 RAY-TRACING EQUATIONS FOR ANISOTROPIC MEDIA

The ray-tracing equations for anisotropic inhomogeneous media can be written in the following form (Červený 1972, Eq. 13; Červený, Molotkov & Pšenčík 1977, Eq. 5.18)

$$\frac{dx_i}{d\tau} = \frac{1}{2}\frac{\partial G}{\partial p_i}, \quad \frac{dp_i}{d\tau} = -\frac{1}{2}\frac{\partial G}{\partial x_i}, \tag{1}$$

where x_i are the components of the position vector, τ is the traveltime, $p_i = \dfrac{\partial \tau}{\partial x_i}$ are the components of the slowness vector, $G = G(x_i, p_i)$ is the eigenvalue of the Christoffel tensor $\Gamma_{jk} = a_{ijkl} p_i p_l$, and a_{ijkl} is the density-normalized elasticity tensor. The eigenvalue G is calculated from the Christoffel equation

$$\det(\Gamma_{jk} - G\delta_{jk}) = 0 \ , \tag{2}$$

which represents a cubic algebraic equation

$$G^3 - PG^2 + QG - R = 0 \, , \tag{3}$$

with coefficients

$$P = \mathrm{tr}\left(\Gamma_{jk}\right),\ Q = \det\left(\Gamma_{jk}\right),\ R = tr\left(\hat{\Gamma}_{jk}\right), \tag{4}$$

where $\hat{\Gamma}_{jk}$ means matrix of cofactors of Γ_{jk}.

The Christoffel tensor Γ_{jk} has three eigenvalues G, which are real-valued and positive, and three eigenvectors **g**. The eigenvalues correspond to three waves (P, $S1$ and $S2$) propagating in anisotropic media, and eigenvectors correspond to polarization vectors of these three waves. Hence, we should determine three systems of rays. If all three eigenvalues of the Christoffel tensor are different for some direction of slowness vector **p**: $G^P \neq G^{S1} \neq G^{S2}$, we speak of the *regular direction in anisotropy*. If any two eigenvalues coincide for some slowness vector **p**, we speak of the *singular direction in anisotropy*. A typical example of the singular direction is the S-wave singularity. If two eigenvalues coincide for all directions of **p**, then the anisotropy degenerates to isotropy.

3 RAY TRACING IN REGULAR DIRECTIONS

To evaluate derivatives $\frac{\partial G}{\partial p_i}$ and $\frac{\partial G}{\partial x_i}$ in the right-hand side of the ray tracing system (1), we can proceed in the following three ways:

1. We find an analytical solution of Eq. (3) and differentiate it. However, this approach can be used only for very simple types of anisotropy, because in a general case the analytical expressions can be quite complicated and evaluating them is not very effective.

2. We differentiate Eq. (3) using the theorem on implicit functions, thus obtaining

$$\frac{dx_i}{d\tau} = \frac{1}{2\hat{D}}\left(G^2\frac{\partial P}{\partial p_i} - G\frac{\partial Q}{\partial p_i} + \frac{\partial R}{\partial p_i}\right),\ \frac{dp_i}{d\tau} = -\frac{1}{2\hat{D}}\left(G^2\frac{\partial P}{\partial x_i} - G\frac{\partial Q}{\partial x_i} + \frac{\partial R}{\partial x_i}\right), \tag{5}$$

where $G = 1$ and $\hat{D}$ is expressed as

$$\hat{D} = 3G^2 - 2PG + Q\ . \tag{6}$$

This system can be rewritten in a more concise form as follows (Červený 1972, Eq. 15; Červený *et al*. 1977, Eq. 5.19)

$$\frac{dx_i}{d\tau} = a_{ijkl}p_l\frac{\hat{D}_{jk}}{\hat{D}},\ \frac{dp_i}{d\tau} = -\frac{1}{2}\frac{\partial a_{jkln}}{\partial x_i}p_k p_n\frac{\hat{D}_{jl}}{\hat{D}}, \tag{7}$$

where $\hat{D}_{jk}$ is the matrix of cofactors of $D_{jk} = \Gamma_{jk} - G\delta_{jk}$,

$$\hat{D}_{11} = (\Gamma_{22} - G)(\Gamma_{33} - G) - \Gamma_{23}^2, \quad \hat{D}_{12} = \hat{D}_{21} = \Gamma_{13}\Gamma_{23} - \Gamma_{12}(\Gamma_{33} - G),$$

$$\hat{D}_{22} = (\Gamma_{11} - G)(\Gamma_{33} - G) - \Gamma_{13}^2, \quad \hat{D}_{13} = \hat{D}_{31} = \Gamma_{12}\Gamma_{23} - \Gamma_{13}(\Gamma_{22} - G),$$

$$\hat{D}_{33} = (\Gamma_{11} - G)(\Gamma_{22} - G) - \Gamma_{12}^2, \quad \hat{D}_{23} = \hat{D}_{32} = \Gamma_{12}\Gamma_{13} - \Gamma_{23}(\Gamma_{11} - G),$$

where $G = 1$ and $\hat{D}$ is defined either by Eq. (6) or as

$$\hat{D} = \mathrm{tr}(\hat{D}_{jk}) = \hat{D}_{11} + \hat{D}_{22} + \hat{D}_{33}.$$

3. Taking into account that matrix $\hat{D}_{jk}$ in (7) can be expressed by eigenvectors g_k of the Christoffel tensor Γ_{jk} as

$$\frac{\hat{D}_{jk}}{\hat{D}} = g_j g_k, \tag{8}$$

we get the following form of the ray-tracing system

$$\frac{dx_i}{d\tau} = a_{ijkl} p_l g_j g_k, \quad \frac{dp_i}{d\tau} = -\frac{1}{2}\frac{\partial a_{jkln}}{\partial x_i} p_k p_n g_j g_l. \tag{9}$$

4 RAY TRACING IN SINGULAR DIRECTIONS

If we calculate rays for waves with coincident eigenvalues, we face with difficulties. Since the Christoffel tensor is degenerate, the denominator term $\hat{D}$ in Eqs (5) and (7) becomes zero. Subsequently, the nominator term in (5) and (7) also becomes zero and right-hand sides of these equations yield indefinite expressions $\frac{0}{0}$. This produces a numerical instability and causes trouble in ray tracing problems. The instability arises not only when two eigenvalues coincide, but also whenever they are very close to each other (Shearer & Chapman 1989, Červený 2000; Pšenčík & Dellinger 2000). Therefore, the equations (5) or (7) are not very appropriate for tracing rays in media with singularities and we shall no more consider them in the next. We can avoid the mentioned difficulties using ray-tracing system (9), which produces no breakdowns in singularities. But this system also needs some modification. Namely, we have to be more accurate when evaluating the polarization vectors of traced waves, which are necessary for the evaluation of right-hand sides of this system. Commonly, the polarization vectors are uniquely determined as eigenvectors of the Christoffel tensor. In

singular directions, however, the eigenvectors for degenerated waves are not unique and we have to specify rules for determining the proper polarization vectors. In the next, we shall attempt to fix these rules for various kinds of singularities.

Interestingly, we meet no difficulties when using Eq. (9) for tracing rays of S waves in *isotropic media*. In isotropy the rhs of (9) is not sensitive to the actual choice of the S-wave polarization vector. Hence any polarization vector perpendicular to the slowness vector is appropriate for evaluating rhs of (9) and transforms (9) into the standard ray tracing system for *S* waves in isotropy (Červený *et al.* 1977, Eq. 3.2):

$$\frac{dx_i}{d\tau} = \beta^2 p_i \ , \ \frac{dp_i}{d\tau} = -\frac{1}{\beta}\frac{\partial \beta}{\partial x_i}, \tag{10}$$

where β is the *S*-wave velocity.

Obviously, a similar situation to isotropy appears when tracing rays of S waves in *very weakly anisotropic media*. In this case, the slowness sheets of S wave almost coincide at all directions and in some directions can be exactly equal. The Christoffel tensor is degenerate or nearly degenerate and the S-wave polarization vectors are generally determined with a low accuracy. Fortunately, the low accuracy of the polarization vectors determined has no effect to a proper tracing of rays for S waves, because of the very weak sensitivity of ray-tracing equations (9) to the actual choice of the polarization vector. Hence the rays in isotropic and very weakly anisotropic media can be traced by (9) without any difficulty.

The next type of singularity to be inspected is a *kiss singularity*. The kiss singularity is defined as the direction, in which two *S*-wave slowness surfaces touch tangentially at an isolated point (see Fig. 1). Consequently, S wavefronts also touch tangentially at the kiss singularity, thus the group velocities for the both S waves coincide being equal to the phase velocity and parallel to the slowness vector at this point. In the vicinity of the singularity, the polarization of *S* waves behaves anomalously (see Fig. 1), and at the singularity the polarization vectors are not defined uniquely. Nevertheless this singularity does not pose serious difficulties to ray-tracing system (9). Similarly to isotropy, the rhs of (9) is insensitive to the actual choice of the S-wave polarization vector in the singularity. If we insert any polarization vector perpendicular to the slowness vector, then the ray-tracing equations (9) take in the singularity the following simple form

$$\frac{dx_i}{d\tau} = c^2 p_i \ , \ \frac{dp_i}{d\tau} = -\frac{1}{c}\frac{\partial c}{\partial x_i}, \tag{11}$$

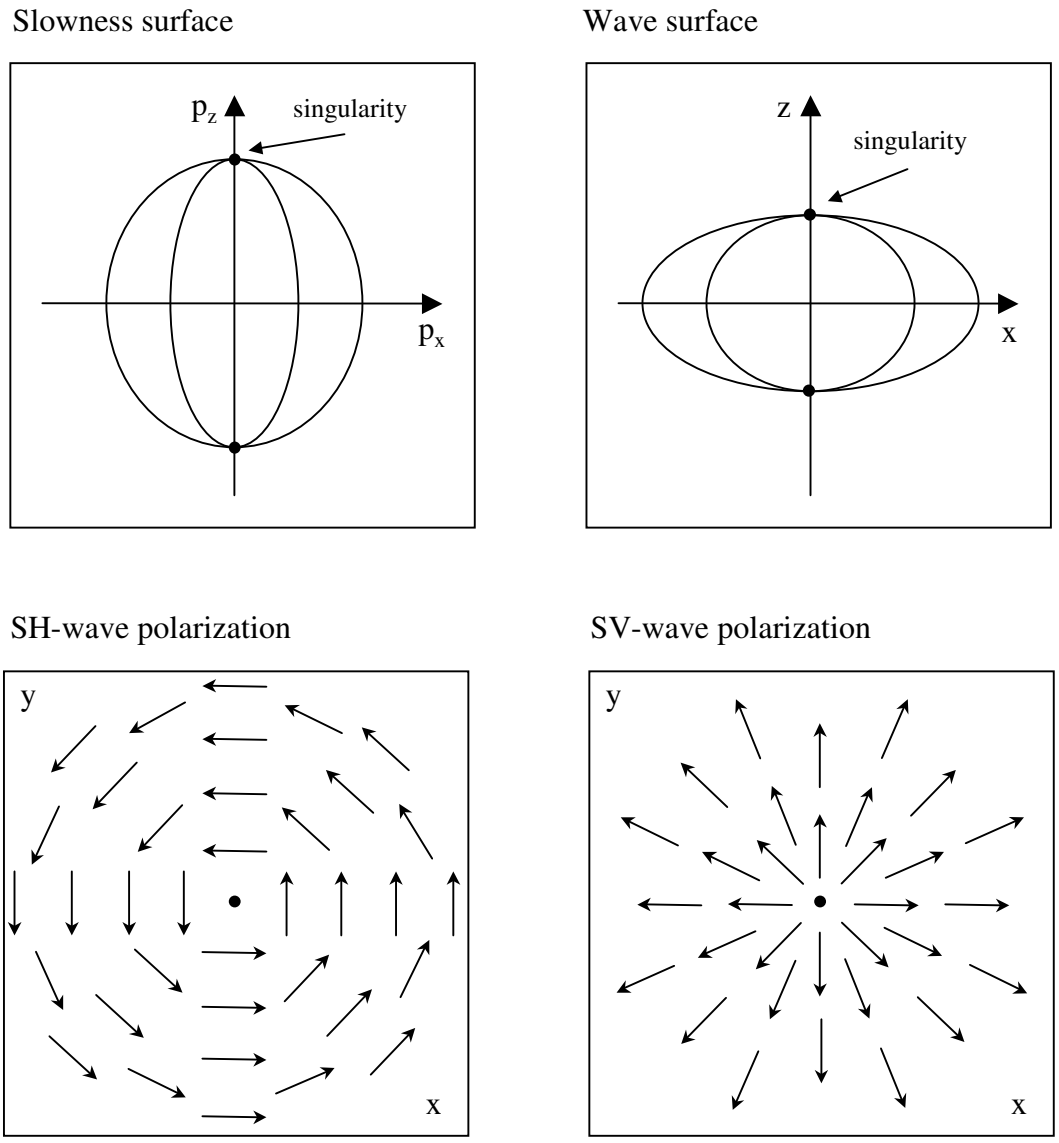

Figure 1. Kiss singularity in transverse isotropy with a vertical axis of symmetry. Upper plots show vertical sections of the slowness and wave surfaces. Lower plots show the horizontal projection of the SH- and SV-wave polarization vectors at the wave surface.

where c is the phase velocity of the *S* waves along the axis of symmetry (the same for both S waves). Since the ray-tracing system is completely independent of the polarization vector of S

wave in the singularity, we can expect that this system will also be almost insensitive to any variation of S-wave polarization vectors in the close vicinity of the singularity. It implies that one should not be afraid of strange or incorrect behaviour of rays due to S-wave polarization anomalies near the kiss singularity.

The difficulties can arise, however, when tracing rays in the vicinity of an intersection singularity. The intersection singularity typically occurs in transversely isotropic (TI) media, where slowness (or phase velocity) surfaces of the S waves can intersect along a line (see Fig. 2). This singular line in the slowness surface splits into two different lines in the wave surface (see Fig. 2, upper right plot). For the singular line, the rhs of (9) depends on the choice of the S-wave polarization vector. Hence this choice has a significant impact on the form of rays calculated. But to find a proper polarization vector for the traced wave is not very complicated. Since the polarization on the slowness surfaces near the singularity changes smoothly (see Fig. 2, lower plots), we can easily associate a proper polarization to the particular traced wave. This has been recognized and successfully applied by Shearer & Chapman (1989) who used in ray tracing (9) analytical formulae for polarization vectors in transverse isotropy. These analytical formulae are valid even in the singularity and guarantee smooth change of the polarization vector along a ray when the ray passes the singularity. If we evaluate the polarization vector numerically as the eigenvector of the Christoffel tensor, we have no unambiguous rule for calculation of the polarization vector in the singularity. However, the numerical approach should follow a similar rule as the analytical approach: *when a ray crosses the singularity, the change of the polarization vector along the ray must be smooth*.

The most complicated singularity in anisotropy is a *conical point*. The conical point (or the point singularity) is defined as the direction, in which two slowness sheets touch through vertices of cone-shaped surfaces (see Fig. 3). Hence, in the vicinity of this singularity the both slowness sheets look like two identical cones placed tip to tip (Crampin & Yedlin 1981; Rümpker & Thomson 1994). The singular point in the slowness sheet generates a singular line in the wave sheet (see Figs 3, 4). Hence all points at the singular line of the wave sheet have the same slowness vector. In other words, a cone of acceptable rays corresponds to one slowness vector at the singular point. In reverse, wave sheets can also form a conical point (point Q at Fig 3). This point generates a line of points in the slowness sheet, which are associated to the same ray direction.

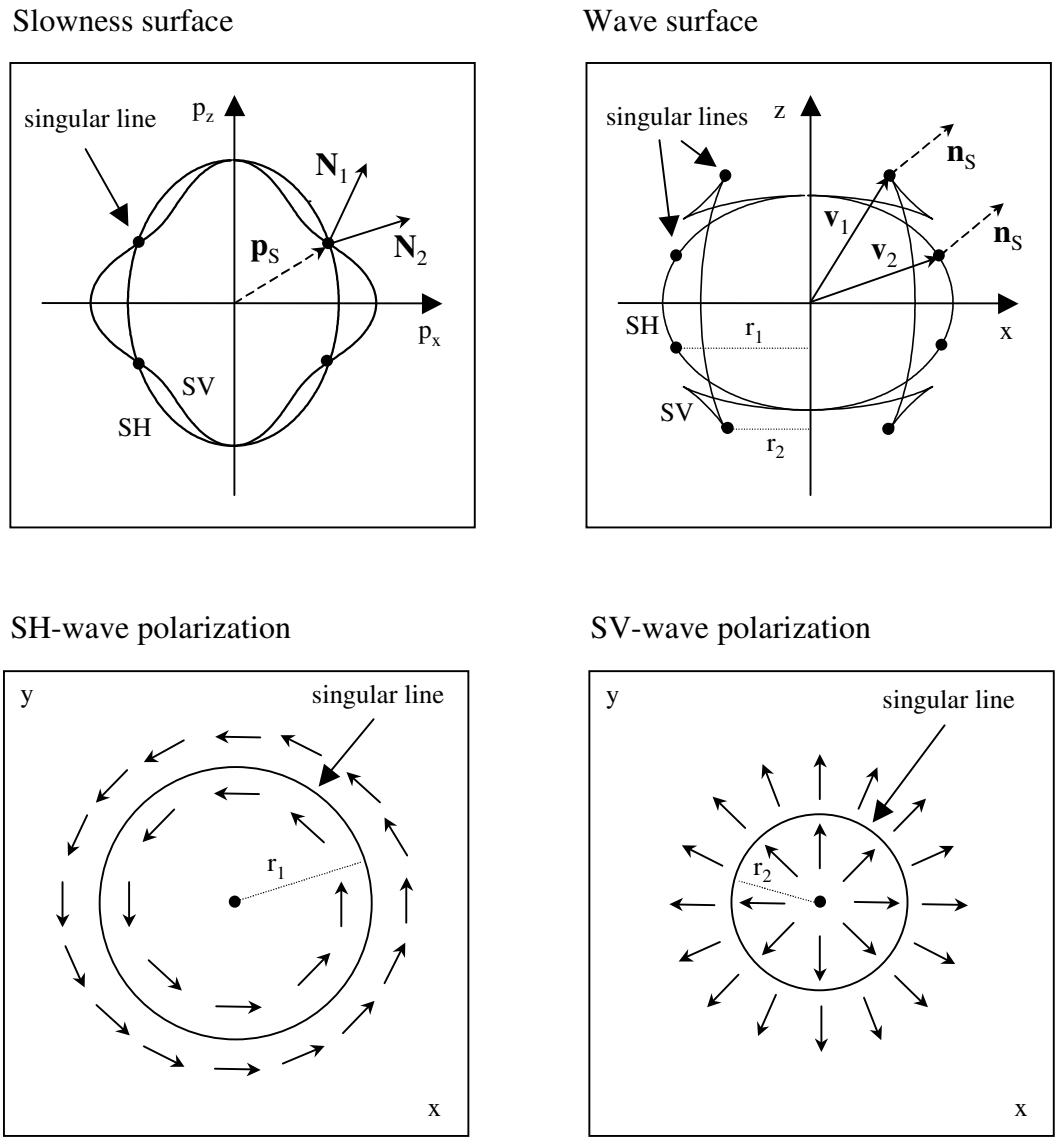

Figure 2. Intersection singularity in transverse isotropy with a vertical axis of symmetry. Upper plots show vertical sections of the slowness and wave surfaces. Lower plots show the horizontal projection of the SH- and SV-wave polarization vectors near singular lines at the wave surface. $\mathbf{p}_S$ is the slowness vector at the singularity, $\mathbf{n}_S$ is its direction, $\mathbf{n}_S = \mathbf{p}_S / p$. Vectors $\mathbf{v}_1$ and $\mathbf{v}_2$ are the group velocities at the singularity, $\mathbf{N}_1$ and $\mathbf{N}_2$ are their directions, $\mathbf{N}_1 = \mathbf{v}_1 / v$, $\mathbf{N}_2 = \mathbf{v}_2 / v$, where $v = v_1 = v_2$. Quantities r_1 and r_2 denote the radii of the singular lines at the wave surface. Parameters of the transverse isotropy used are described in Sec. 7.1.

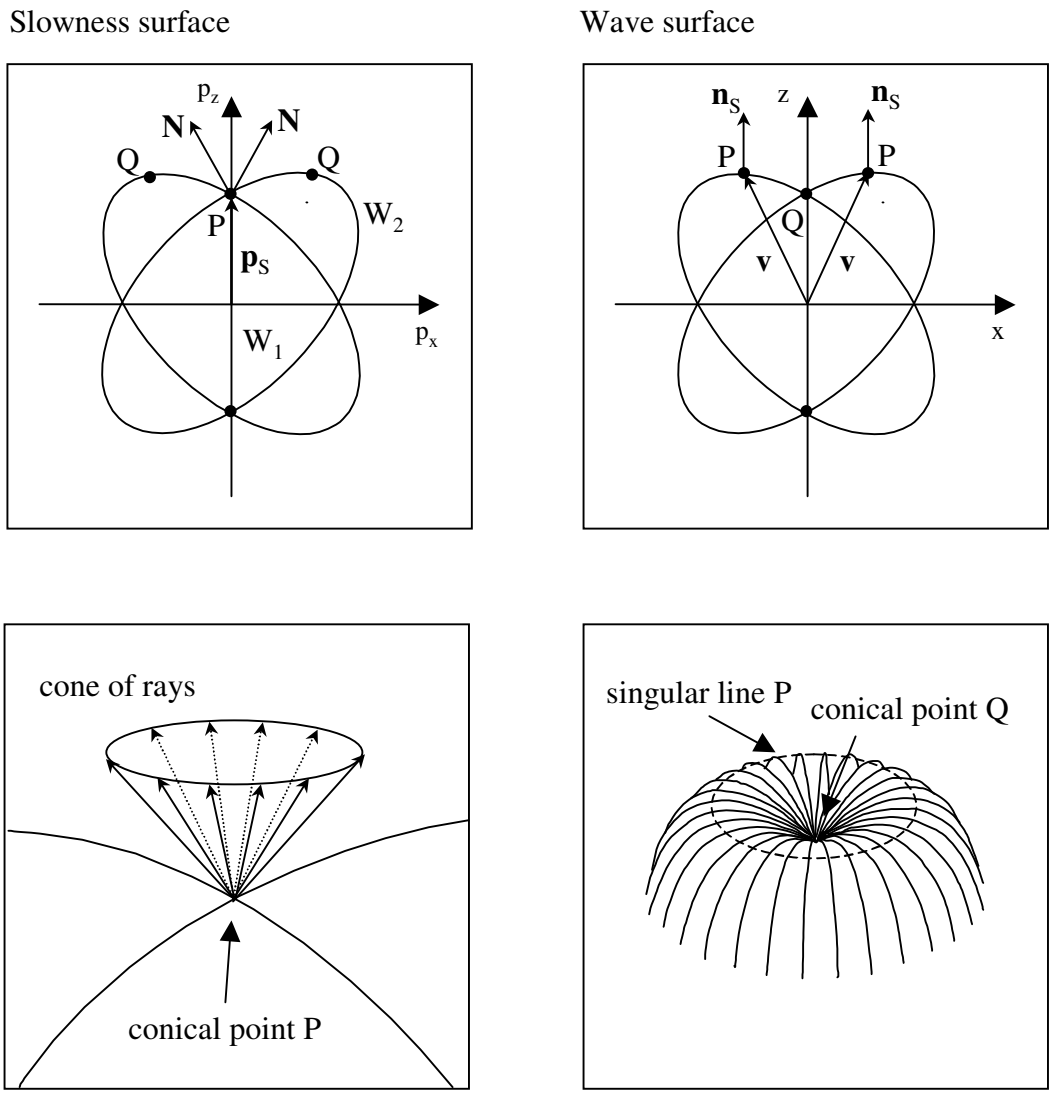

Figure 3. Conical point in the Payton's transverse isotropy (Payton 1992). Upper plots show vertical sections of the slowness and wave surfaces of the W_1 and W_2 waves. Lower plots show a 3-D sketch of the cone of rays generated at the singularity (left-hand plot) and the form of the wave surface near the singular line (right-hand plot). P denotes the singularity, Q is the conical point at the wave surface. For meaning of the other quantities see caption of Fig. 2.

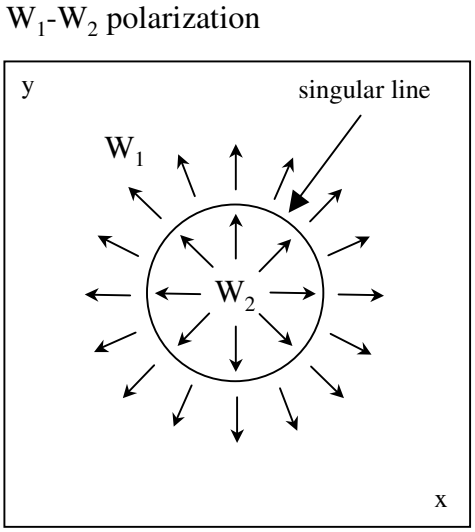

Figure 4. The horizontal projection of the W_1- and W_2-wave polarization vectors near the singular line at the wave surface.

Despite the complexity of the geometry of the conical point, we have to point out that the behaviour of polarization vectors near the singular line in the wave sheet is surprisingly simple. The polarization vectors behave regularly at both sides of the singular line and the polarization pattern is similar to that for the intersection singularity. Hence we can assign the proper polarization of the wave at the singular line in the same way as for the intersection singularity: *we require a smooth change of the polarization along a ray when the ray crosses the singularity*.

Note that the order of waves is interchanged when the ray crosses the singularity: the faster wave in front of singularity becomes the slower wave behind the singularity and *vice versa*.

5. GENERAL STRATEGY FOR RAY TRACING

In the previous section we have discussed behaviour of the ray tracing equations for several particular types of singularity. Now we generalize these results and draw the following strategy for tracing rays in media with any kinds of singularities.

1. The ray reaches a regular point.

The polarization vector of the traced wave is calculated as the eigenvector of the Christoffel tensor. From three eigenvectors calculated we choose that eigenvector which guarantees a smooth change of the polarization vector from the previous to the current point of the ray. We emphasize that it is not sufficient to keep the type of the wave (P, S1 or S2) in the ray tracing procedure. Since a singularity can appear between the previous and the current point of the traced ray, the type of the traced wave can be changed.

Determining a proper polarization vector we can evaluate the rhs of the ray tracing equations and we trace the ray to the next point.

2. The ray touches a singularity.

The polarization vector of the traced wave is not determined by the Christoffel equation uniquely. Therefore, we calculate the polarization vector as a limit of polarization vectors at points of the ray just before the ray touches the singularity (see Fig. 5)

$$\mathbf{g}^{+}(\tau_S) = \lim_{\tau \to \tau_S^{+}} \mathbf{g}(\tau) , \tag{12}$$

where τ is the traveltime along a ray and τ_S means the traveltime at the singularity. Inserting polarization vector $\mathbf{g}^{+}(\tau_S)$ into the ray-tracing equations we move forward to the next point of the ray.

3. The ray leaves the singularity.

Here, we assume two alternatives.

(a) The next point behind the singularity is regular.

In this case, the polarization vectors of the waves degenerated in the singularity are now determined in the standard way by the Christoffel equation. But we have to check, if the ray is split in the singularity or not. To identify this case, we have to determine polarization vectors of the waves, which degenerated in the singularity, also behind the singularity. Then we calculate the limit of polarization vectors along a ray when going backward to the singularity

$$\mathbf{g}^{-}(\tau_S) = \lim_{\tau \to \tau_S^{-}} \mathbf{g}(\tau) , \tag{13}$$

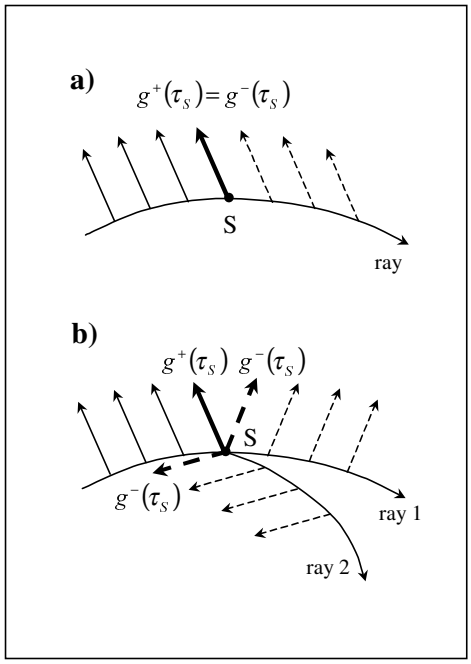

Figure 5. Behaviour of polarization vectors along the ray touching the singularity. (a) The ray does not split in the singularity. (b) The ray splits into two rays in the singularity. Point S denotes the singularity. Full and dashed arrows show the polarization in front of and behind the singularity, respectively. Bold arrows show the polarization in the singularity.

If the polarization vector for one of the degenerated waves behind the singularity matches continuously the polarization of the wave in front of the singularity

$$\mathbf{g}^-(\tau_S)=\mathbf{g}^+(\tau_S)\ , \tag{14}$$

then the ray does not split and we trace the ray for this particular wave (see Fig. 5a). In the other case, we have to trace rays for all waves degenerated in the singularity (see Fig. 5b).

(b) The next point behind the singularity is again singular.

We consider two cases when this situation can arise. First, when the ray touches the singularity, the wave starts to propagate in a homogeneous anisotropic medium. Since the ray becomes a straight line, the wave cannot leave the singularity until an inhomogeneity occurs.

Second, when the ray plunges into a locally isotropic (homogeneous or inhomogeneous) region. In the both mentioned cases we can apply the polarization vector determined at the previous singular point for the tracing of a ray to the next point. In isotropy, we can also switch to a simpler ray-tracing system (10) designed for this medium.

6. NUMERICAL EXAMPLES I: SPLITTING OF RAYS

In this section we shall apply the proposed ray tracing strategy on two medium models. In both models, a singularity occurs along a plane interface, which separates media with different types of anisotropy. In the first model, the interface separates isotropic and anisotropic layers; in the second model, the interface separates two anisotropic layers. The velocities are continuous functions across the interface, hence the interface generates no scattered waves. Nevertheless, we shall show that all rays incident at the interface split into two different rays.

6.1. Isotropy/anisotropy transition

The model consists of two layers: the upper layer is transversely isotropic with a vertical axis of symmetry (VTI layer), the lower layer is isotropic. Both layers are vertically inhomogeneous. The interface is at the depth of 4 km. The point source is situated at the isotropic layer at the depth of 8 km. The P-wave velocities at the source and at the interface are $\alpha = 5.5$ km/s and 4.5 km/s, respectively. The S-wave velocity in the isotropic layer is $\beta = \alpha/\sqrt{3}$. The P- and S-wave velocities in the isotropic layer linearly increase with the depth. The VTI in the upper layer is defined by the density-normalized elastic parameters as follows: $a_{11} = a_{22} = a_{33}$, $a_{13} = a_{23} = a_{11} - 2a_{44}$, $a_{44} = a_{55}$, $a_{66} = a_{44} + 2\varepsilon_3$, $a_{12} = a_{11} - 2a_{66}$. The values of these parameters are at the interface: $a_{11} = 20.25$, $a_{44} = a_{11}/3$ and $\varepsilon_3 = 0$, and at the surface: $a_{11} = 12.25$, $a_{44} = a_{11}/3$ and $\varepsilon_3 = 1$. The anisotropy is controlled by anisotropy parameter ε_3 (see Vavryčuk 1997). This parameter is zero at the interface and linearly increases to the surface. Hence the medium is isotropic at the interface and the anisotropy gradually increases to the surface. The P and SV waves have directionally independent velocities: $\alpha = \sqrt{a_{11}}$, $\beta = \sqrt{a_{44}}$, which linearly increase with the depth. For the S-wave

velocities at the surface see Fig. 6. Rays of the S wave are shot from the point source in the angle interval $\theta \in \langle 0°, 90° \rangle$ with the step of 10°.

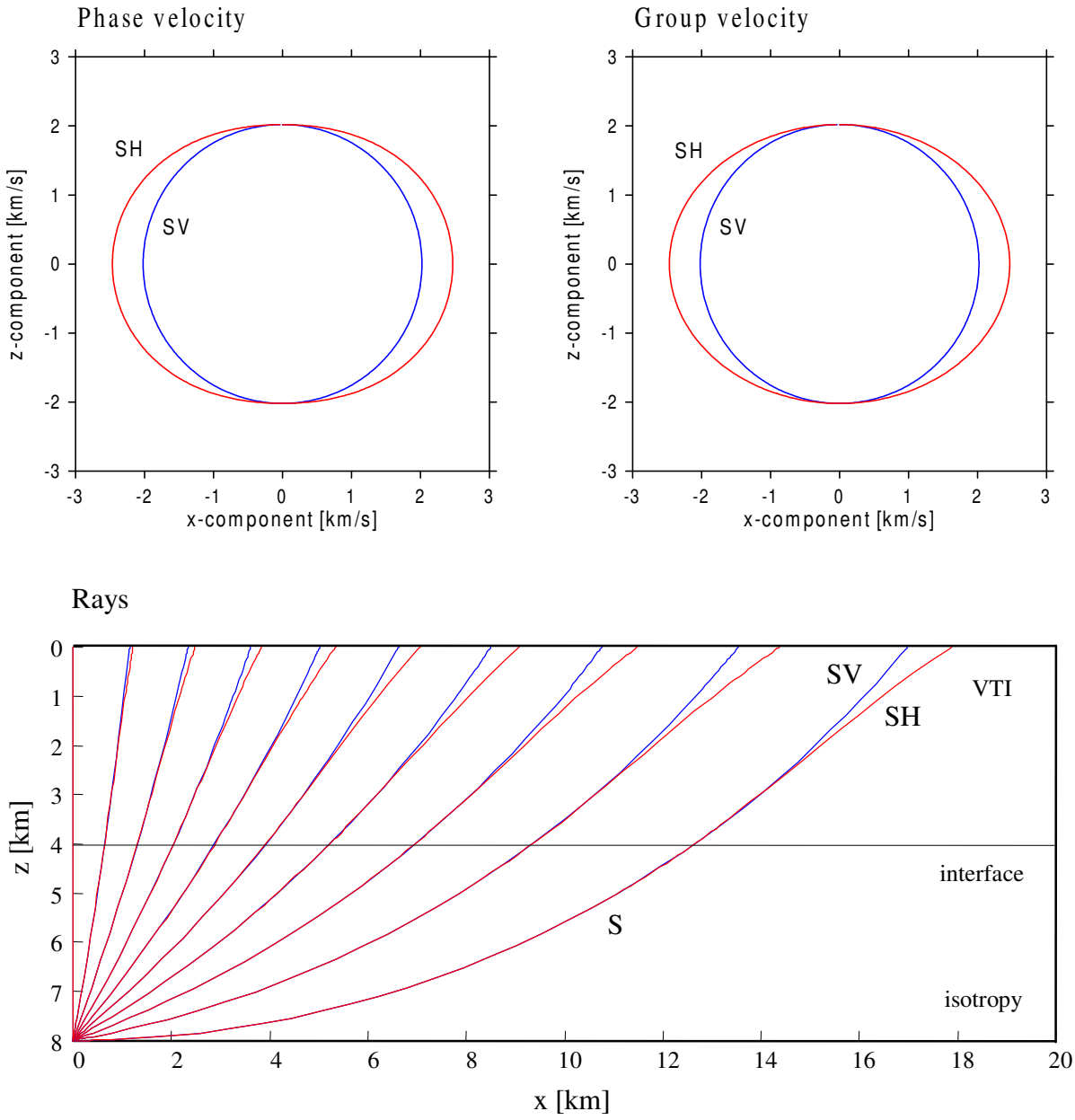

Figure 6. Splitting of rays of the S waves at the isotropy/VTI transition. Upper plots show the vertical sections of the phase and group S-wave velocities of the VTI medium at the surface. The lower plot shows rays in the medium. For parameters of the isotropic and VTI layers see the text.

Since the transition between the isotropic and the VTI layers is smooth, no scattered waves are generated at the interface. Despite this fact, the rays split at the interface (see Fig. 6, lower plot), because the interface separates the singular and regular anisotropic regions. Since the anisotropy is VTI, the S wave splits into the SV and SH waves. The splitting of the SV and SH rays is smooth, because the tangent of the split rays is the same for both rays at the interface. The deviation between the rays of split waves increases with increasing anisotropy of the VTI layer. If the source generates the S wave with polarization of the SV or SH wave, then no splitting occurs at the interface.

6.2 Anisotropy/anisotropy transition

This model consists of two transversely isotropic layers: the upper layer has a vertical axis of symmetry (VTI), the lower layer has a horizontal axis of symmetry (HTI), which deviates from the *x*-axis by 45°. The transverse isotropy of the HTI layer is essentially the same as for the VTI layer. The difference is only in the orientation of the axis of symmetry. The parameters of HTI in the local coordinate system, which has the symmetry axis parallel to the *z*-axis, are at the source: $a_{11} = 30.25$, $a_{44} = a_{11}/3$ and $\varepsilon_3 = 1$, and at the interface: $a_{11} = 20.25$, $a_{44} = a_{11}/3$ and $\varepsilon_3 = 0$. The P and SP waves have velocities, $\alpha = \sqrt{a_{11}}$, $\beta = \sqrt{a_{44}}$, which linearly increase with the depth. The parameters of the VTI layer are the same as for the isotropy/VTI model. Also the positions of the source and of the interface are similar to the isotropy/VTI model. Anisotropy parameter ε_3 linearly decreases in the HTI layer from unity at the source depth to zero at the interface. Hence both HTI and VTI layers are in fact isotropic at the interface. The strongest anisotropy is observed at the depth of the source and at the surface, but the anisotropies have a different orientation.

Figure 7 shows results of the ray tracing of two S waves (denoted SR and SP waves) generated at the source. Likewise in the isotropy/VTI model, the interface represents the singular region in the HTI/VTI model. Since the orientation of anisotropy is different on both sides of the singularity, the rays of each S wave split at the singularity. Figure 7 shows the splitting of both SP and SR waves separately (upper and lower plots).

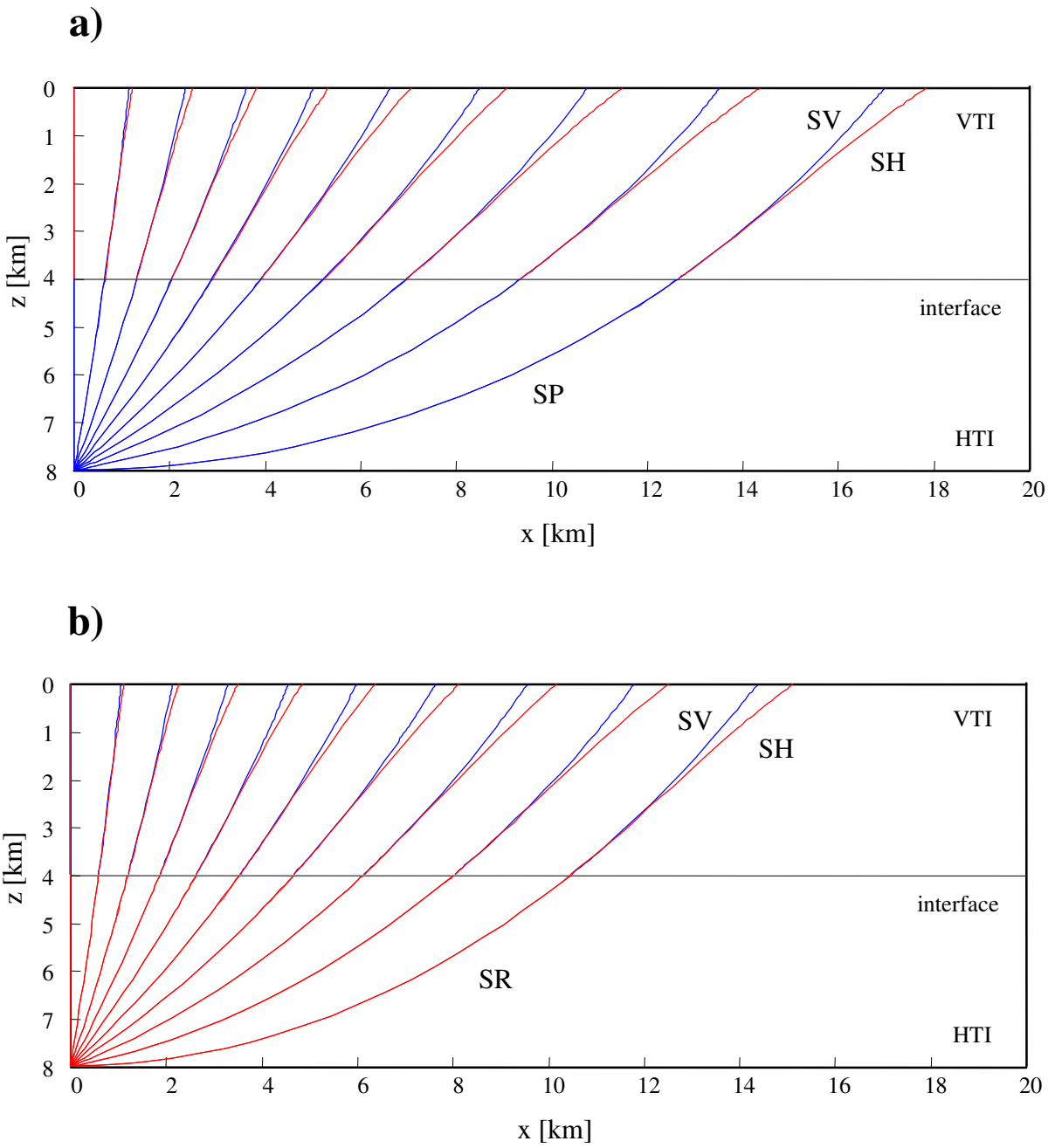

Figure 7. Splitting of rays of the S waves at the HTI/VTI transition. (a) Ray tracing for the faster S wave generated at the source. (b) Ray tracing for the slower S wave generated at the source. SP wave is that S wave, which has a polarization vector perpendicular to a ray and to the symmetry axis. SR wave has a polarization vector lying in the plane of a ray and the symmetry axis.

7. NUMERICAL EXAMPLES II: FALSE BENDING OF RAYS

In this section we shall apply the ray tracing strategy to the vertically inhomogeneous media containing the intersection singularity and the conical point. We shall demonstrate how important is a proper determination of polarization vectors of traced waves in the singularity and in its vicinity. We shall show that neglecting of rules discussed in the previous section can lead to a false ray tracing. The false ray tracing is namely manifested by an abrupt change of the ray direction in the singularity. This false bending of rays can be easily corrected when calculating correct polarization vectors at and behind the singularity.

7.1. Intersection singularity

For tracing of rays near the intersection singularity we applied a similar model to "Model 4" introduced and studied by Shearer & Chapman (1989). This model is extremely anisotropic. Our model displays the same type of anisotropy, but instead of the horizontal axis of symmetry we use the vertical axis of symmetry. Hence the elastic parameters of the medium are: $a_{11} = 19.63$, $a_{22} = a_{33} = 20.16$, $a_{44} = 6.38$, $a_{55} = a_{66} = 3.48$, $a_{12} = a_{13} = 7.26$, $a_{23} = a_{33} - 2a_{44}$. These parameters are referred to the depth of the source $z_0 = 8$ km. The elastic parameters at other depths were calculated as:

$$a_{kl} = a_{kl}(z_0)\left[1 + \varepsilon(z - z_0)\right]^2 \ , \tag{15}$$

where $\varepsilon = 0.04\,\mathrm{km}^{-1}$ is the normalized velocity gradient in the medium. The rays of the S waves were shot in the x_1-x_3 plane in the following intervals of angles: $\theta \in \langle 22°, 46° \rangle$ with the step of 2° for the slower S wave, and $\theta \in \langle 16°, 52° \rangle$ with the step of 2° for the faster S wave, where θ means the deviation of the slowness vector from the vertical axis.

Figure 8 shows sections of the phase and group velocities at the source and the results of the ray tracing. The intersection singularity at the phase surface is split into two singular lines at the wave surface. Moreover, one of the singular lines coincides with the edge line due to a triplication. Although the geometry of the wave surface looks complicated, the correct ray tracing does not pose serious difficulties. The only problem arises in the singularity, where we require a continuous change of the direction of the polarization vector of the traced wave along a ray. This requirement is important, because the order of waves is interchanged in the singularity: the slower wave becomes faster and the faster wave becomes slower. If we neglect this fact and assume that the wave should be faster (or slower) along an entire ray, then we obtain spurious results. The change of the polarization vector is discontinuous in the singularity and we observe a false abrupt change of the direction of the ray (see Fig. 8, middle plots). Obviously, correct ray tracing (see Fig. 8, lower plots) yields smooth curved rays, as it should be in smoothly varying inhomogeneous media.

7.2. Conical point

For tracing of rays near the conical point, we use a medium displaying cubic anisotropy. The cubic anisotropy is defined by the following elastic parameters: $a_{11} = a_{22} = a_{33}$, $a_{44} = a_{55} = a_{66}$, $a_{12} = a_{13} = a_{23} = a_{11} - 2a_{44} + \delta$, where δ is the parameter measuring the strength of anisotropy. We adopted the following values for the elastic parameters at the source, $a_{11} = 6.25$, $a_{44} = a_{11}/3$, $\delta = 2.00$. Elastic parameters at other depths were calculated by Eq. (15) with the value of the velocity gradient $\varepsilon = 0.01$ km^{-1}. Similarly to the previous models, the source is situated at the depth of 8 km. The conical point in the cubic anisotropy is defined by the slowness vector with the spherical angles: $\varphi = 45°$ and $\theta = 54.74°$. It implies that the conical point does not lie in the *x*-*z* plane. Therefore, the rays of the S waves are shot in the plane, which deviates from the *x*-*z* plane by the angle $\varphi = 45°$, in the following intervals of angle θ: $\theta \in \langle 44°, 69° \rangle$ with the step of 1° for the S faster wave outgoing from the source, and $\theta \in \langle 55°, 70° \rangle$ with the step of 1° for the slower S wave outgoing from the source.

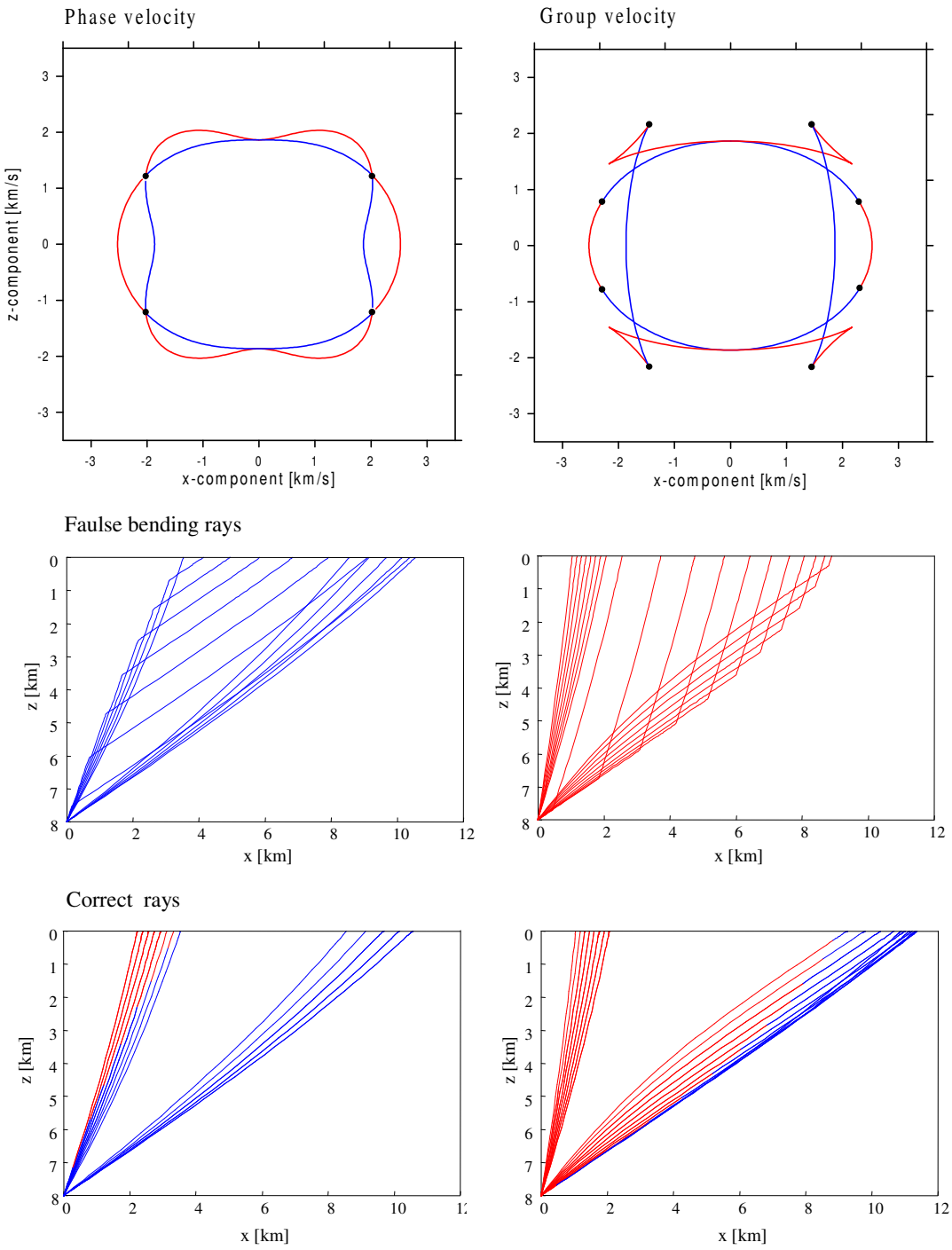

Figure 8. Ray tracing of the S waves across the intersection singularity in the VTI medium. Upper plots show the vertical sections of the phase and group S-wave velocities. The middle plots show a false bending of rays crossing the singularity. The lower plots show correct ray tracing across the singularity. Red line – faster S wave, blue line – slower S wave. The dots in the velocity plots denote the singularity.

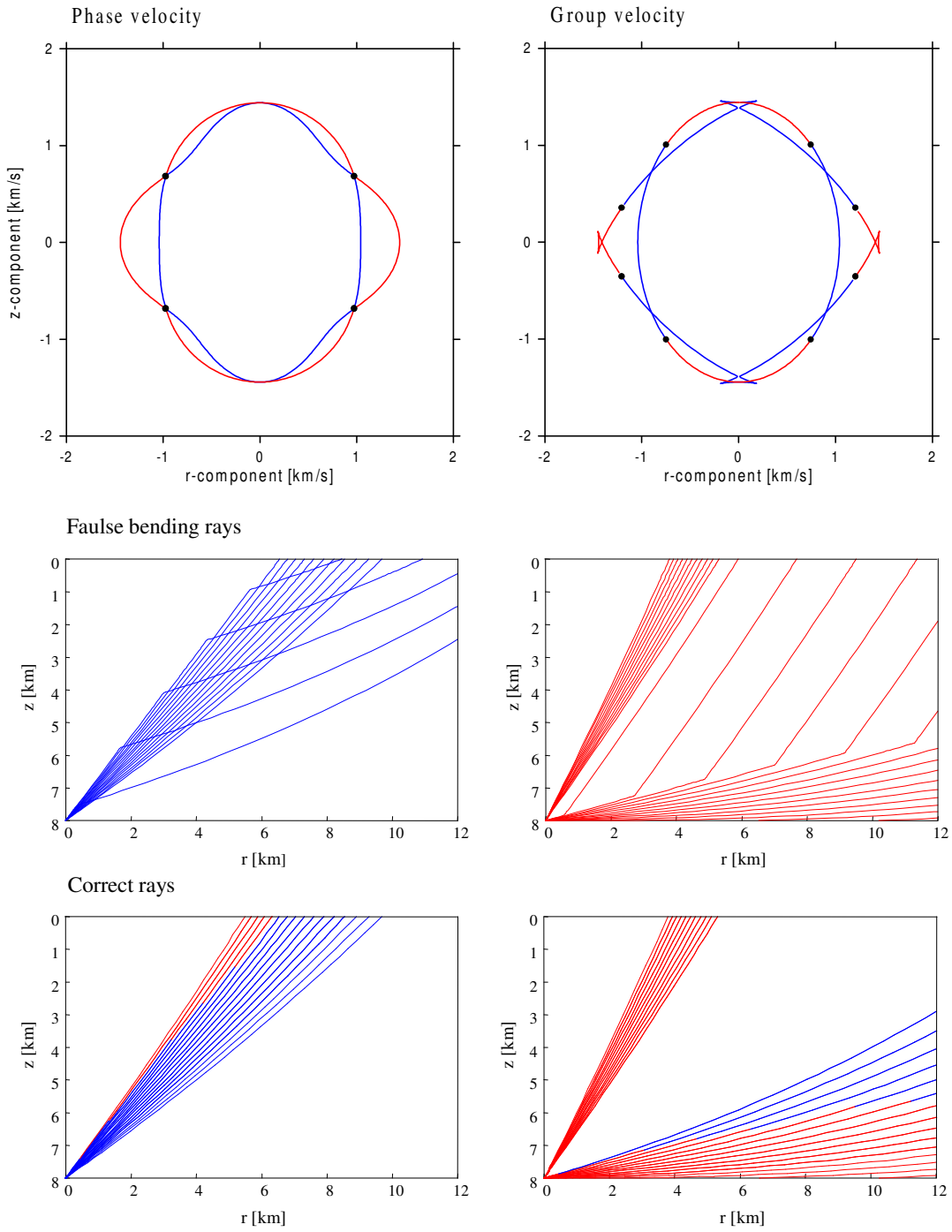

Figure 9. Ray tracing of S waves across the conical point in cubic anisotropy. Axis r is horizontal and deviates from the x-axis by angle $\varphi = 45°$. For other details, see the caption of Fig. 8.

The sections of the phase and group velocities at the source and the results of the ray tracing are shown in Fig. 9. Neither the phase velocities nor the group velocities are axially symmetric in cubic anisotropy like in the transverse isotropy (see Fig. 8). Therefore, the four points in the phase velocity section really represent four point singularities. The eight points in the group velocity section represent a section of four singular circles (for a geometry of the singular line see Fig. 3). Although the geometry of the conical point is more complicated than the geometry of the intersection singularity, the ray tracing results are in both types of singularity essentially same. If we do not take into account the fact that the polarization vectors must be continuous along a ray, then the rays abruptly bend in the singularity. If we interchange the type of the traced wave in the singularity (S1 to S2 and S2 to S1) because of continuity of the polarization vector of the traced wave, then the rays are smooth and the abrupt ray bending disappears. The situation significantly changes, however, if rays come very near the singularity, but they do not cross it. Figure 10 shows ray tracing when the rays are not strictly in the plane of the singularity being shot with the same values of the deviation angle θ, but in the azimuth $\phi = 47°$. In this case, the ray cannot touch the singularity and the wave type (S1 or S2) remains unchanged for the entire ray. Since the curvature of the phase velocity sheet is near the singularity very high, the ray can be significantly bent even if the velocity gradient in the medium is very weak. This situation also demands a high accuracy of calculated polarization vectors because of extreme sensitivity of the ray direction to the polarization in this particular region. However, this bending occurs only in strongly anisotropic media and it is localised to a close vicinity of the conical point. Moreover, the ray bending is always smooth (see Fig. 10, lower plots). For weakly anisotropic media, this effect disappears.

8 CONCLUSION

We have proposed and tested a strategy for ray tracing in anisotropic inhomogeneous media, which is applicable even in the S-wave singular directions and their vicinities. This ray tracing is numerically stable and yields correct results for all the following troubling situations: for a transition between isotropy and anisotropy, for a very weak anisotropy and for all kinds of singularity in strong anisotropy.

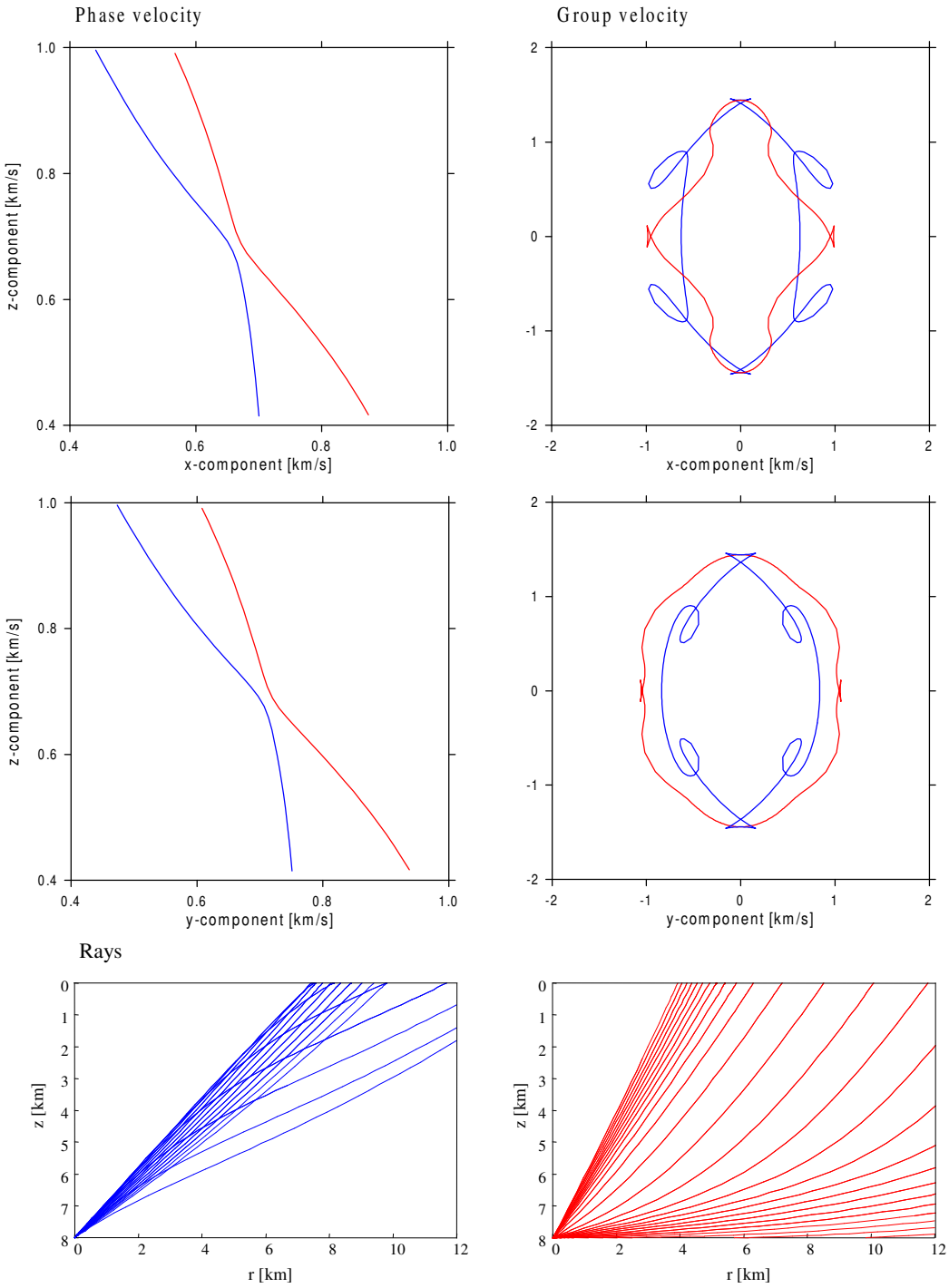

Figure 10. Ray tracing of S waves near the conical point in cubic anisotropy. Upper plots and middle plots show the *x*-*z* and *y*-*z* sections of the phase and group S-wave velocities, respectively. The phase velocities are shown only near the point where the S velocity sheets almost touch. Lower plots show bending of rays near the singularity. Axis *r* is horizontal and deviates from the *x*-axis by angle $\varphi = 47°$. Since the rays are not planar, the lower plots show only projections of the rays.

The ray tracing equations are based on evaluation of their right-hand sides by means of the polarization vector of the traced wave. This approach does not pose any difficulty when tracing rays in transition areas between isotropy and anisotropy, in areas of very weak anisotropy and also in directions of the kiss singularity. However, a special attention has to be paid to the behaviour of the polarization vector of traced waves near and in the intersection singularity and the conical point. In these cases, we have to impose an additional condition requiring the polarization vector of the traced wave to be a continuous function along the ray. If we do not treat with the polarization vector in this way, then the ray tracing can produce abrupt changes of the direction of the ray in the singularity. But the abrupt bending of a ray is unphysical in the smoothly varying inhomogeneous media. The incorrectness of this bending is clear for the intersection singularity, but less obvious for the conical point, because the conical point displays a complicated geometry in both the phase and wave surfaces. Moreover, the geometry of rays can really be significantly distorted be the presence of the conical point in anisotropy. This happens namely in strong anisotropy, when the ray approaches the conical point passing it with no touching. This can produce a substantial bending of rays, but this bending is always smooth and the polarization vector of the traced wave is continuous along the ray. In particular cases, we can also observe that the ray is split in the singularity. This appears if the symmetry of anisotropy behind the singularity is different from that in front of the singularity. This is the case of smooth transitions between isotropy and anisotropy. It can also be frequently observed in very weak anisotropy, where a small perturbation of elastic parameters can lead to a rapid change of the orientation of anisotropy or to a change of anisotropy itself. As regards the strong anisotropy, we assume that the splitting in the singularity is not a frequent case.

Acknowledgements. I thank Ivan Pšenčík for critically reading the manuscript and offering his comments. The work was supported by the Grant Agency of the Czech Republic, grant 205/00/1350, by the Consortium project “Seismic waves in complex 3-D structures”, and by the project “Propagation of seismic waves in singular directions of anisotropic media” supported by CNPq, Brazil.

References

Alshits, V.I. & Lothe, E., 1979. Elastic waves in triclinic crystals. Topology of polarization fields and some general theorems, *Crystallography*, **24**, 683-693 (in Russian).

Alshits,V.I., Sarychev, A.V. & Shuvalov, A.L., 1985. Classification of the degenerations and analysis of their stability in elastic wave theory in crystals, *J. Exper. Theor. Phys.*, **89**, 922-938 (in Russian).

Burridge, R., 1967. The singularity on the plane lids of the wave surface of elastic media with cubic symmetry, *Q. J. Mech. appl. Math.*, **20**, 41-56.

Červený, V., 1972. Seismic rays and ray intensities in inhomogeneous anisotropic media, *Geophys. J. R. astr. Soc.*, **29**, 1-13.

Červený, 2000. *Seismic Ray Theory*, Cambridge University Press, Cambridge, in print.

Červený, V., Molotkov, I.A. & Pšenčík, I., 1977. *Ray Method in Seismology*, Charles University Press, Praha.

Crampin, S. & Yedlin, M., 1981. Shear-wave singularities of wave propagation in anisotropic media, *J. Geophys.*, **49**, 43-46.

Gajewski, D. & Pšenčík, I., 1990. Vertical seismic profile synthetics by dynamic ray tracing in laterally varying layered anisotropic structures, *J. Geophys. Res.*, **95**, 11.301-11.315.

Grechka, V.Yu. & Obolentseva, I.R., 1993. Geometrical structure of shear wave surfaces near singularity directions in anisotropic media, *Geophys. J. Int.*, **115**, 609-616.

Helbig, K., 1994. *Foundations of anisotropy for exploration seismics*, Pergamon, New York.

Miller, G. F. & Musgrave, M.J.P., 1956. On the propagation of elastic waves in aelotropic media. III. Media of cubic symmetry, *Proc. R. Soc. Lond.*, **A**, **236**, 352-383.

Musgrave, M.J.P., 1985. Acoustic axes in orthorhombic media, *Proc. R. Soc. Lond.*, *A*, **401**, 131-143.

Payton, R.G., 1992. Wave propagation in a restricted transversely isotropic elastic solid whose slowness surface contains conical points, *Q. J. Mech. Appl. Math.*, **45**, 183-197.

Pšenčík, I. & Dellinger, J., 2000. Quasi-shear waves in inhomogeneous weakly anisotropic media by the quasi-isotropic approach: a model study, *Geophysics*, accepted.

Rümpker, G. & C. J. Thomson, 1994. Seismic-waveform effects of conical points in gradually varying anisotropic media, *Geophys. J. Int.*, **118**, 759-780.

Shearer, P. M. & C. H. Chapman, 1989. Ray tracing in azimuthally anisotropic media – I. Results for models of aligned cracks in the upper crust, *Geophys. J. Int.*, **96**, 51-64.

Vavryčuk, V., 1997. Elastodynamic and elastostatic Green tensors for homogeneous weak transversely isotropic media, *Geophys. J. Int.*, **130**, 786-800.

Vavryčuk, V., 1999. Properties of S waves near a kiss singularity: a comparison of exact and ray solutions, *Geophys. J. Int.*, **138**, 581-589.